Journal of Human Evolution 59 (2010) 595–607

Contents lists available at ScienceDirect

Journal of Human Evolution

journal homepage: www.elsevier.com/locate/jhevol

The bony labyrinth of the early platyrrhine primate *Chilecebus*

Xijun Ni [a,b,c,*], John J. Flynn [a,c,d], André R. Wyss [e]

[a] Division of Paleontology, American Museum of Natural History, Central Park West at 79th Street, New York, NY 10024, USA
[b] Laboratory of Evolutionary Systematics of Vertebrates, Institute of Vertebrate Paleontology and Paleoanthropology, Xi Zhi Men Wai Street 142, Beijing 100044, PR China
[c] New York Consortium in Evolutionary Primatology, Anthropology PhD Program, CUNY Graduate School, 365 5th avenue, New York, NY 10016, USA
[d] Richard Gilder Graduate School, American Museum of Natural History, Central Park West at 79th Street, New York, NY 10024, USA
[e] Department of Earth Science, University of California—Santa Barbara, Santa Barbara, CA 93106, USA

ARTICLE INFO

Article history:
Received 3 October 2008
Accepted 25 June 2010

Keywords:
Chilecebus carrascoensis
Cochlea
Semicircular canal

ABSTRACT

We document the morphology of the bony labyrinth of *Chilecebus carrascoensis*, one of the best preserved early platyrrhines known, based on high resolution CT scanning and 3D digital reconstruction. The cochlea is low and conical in form, as in other anthropoids, but has only 2.5 spiral turns. When the allometric relationship with body mass is considered, cochlear size is similar to that in extant primates. The relative size of the semicircular canals, which is well within the range of other primates, indicates that *Chilecebus carrascoensis* was probably not as agile in its locomotion as other small-bodied platyrrhines such as *Leontopithecus rosalia*, *Saguinus oedipus*, and *Callithrix jacchus*, but it probably was not a suspensory acrobat or a slow climber. The proportion, shape, and orientation of the semicircular canals in *Chilecebus carrascoensis* also mirror that typically seen in extant primates. However, no single variable can be used for predicting the locomotor pattern in *Chilecebus carrascoensis*. Based on Principle Component Analysis (PCA) scores we calculated rescaled Euclidean distances for various taxa; primates with similar locomotor patterns tend to share shorter distances. Results for *Chilecebus carrascoensis* underscore its general resemblance to living quadrupedal primate taxa, but it is not positioned especially near any single living taxon.

Introduction

The gross anatomy of the bony labyrinth, where the organs of hearing and balance are located, has strong correlations with hearing capability and locomotor specialization in extant mammals (Jones and Spells, 1963; Spoor and Zonneveld, 1998; Spoor et al., 2007; Manoussaki et al., 2008). These correlations could have important implications for understanding the evolution of mammalian hearing and balance (Meng and Wyss, 1995; Spoor and Zonneveld, 1998; Spoor et al., 2002, 2007; Manoussaki et al., 2008; Walker et al., 2008; Silcox et al., 2009).

Almost nothing is known about the bony labyrinth in basal platyrrhines. This paper presents one component of the detailed description of the basicranium of the Miocene fossil platyrrhine *Chilecebus carrascoensis*. We document the morphology of the bony labyrinth of this taxon, one of the best preserved early platyrrhines, based on high resolution computed tomography (CT) scanning and 3D digital reconstruction. The only known specimen of this taxon (SGOPV 3213) is a nearly complete skull discovered in volcaniclastic deposits of the Abanico (Coya-Machalí) Formation in the Andes of central Chile. A high-precision $^{40}Ar/^{39}Ar$ date of 20.09 ± 0.27 Ma is directly associated with the fossil (Flynn et al., 1995). While this anthropoid taxon is more closely related to crown platyrrhines than to catarrhines or stem anthropoids, its precise phylogenetic position has not yet been assessed in detail (e.g., lying within crown clade Platyrrhini or a more basal member of the platyrrhine stem lineage; Wyss and Flynn, 1994; Flynn et al., 1995). To reflect this phylogenetic uncertainty, and because there is not yet a commonly accepted formal taxonomic name for the more inclusive clade of crown Platyrrhini plus stem platyrrhines, we refer to *Chilecebus carrascoensis* by the informal term "platyrrhine."

Materials and methods

High resolution X-ray CT scans

CT scanning was performed at the Center for Quantitative Imaging at Pennsylvania State University. The data set obtained for *Chilecebus carrascoensis* yields a 16-bit grayscale volume in TIFF format. This

* Corresponding author.
E-mail address: nixijun@ivpp.ac.cn (X. Ni).

0047-2484/$ – see front matter © 2010 Elsevier Ltd. All rights reserved.
doi:10.1016/j.jhevol.2010.06.008

image stack of 1148 individual slices includes 1024 × 1024 × 1148 voxels, each voxel having a dimension of 0.04000 × 0.04000 × 0.04641 mm^3.

3D visualization

The Half Maximum Height method (Baxter and Sorenson, 1981; Spoor et al., 1993) was used to assist in identifying the bone–matrix interface. Since the maximum grayscale value of bone in the CT images varies, various thresholds are dynamically measured rather than using a single threshold for processing the entire image stack. The sinuses and spongy bone cavities surrounding the bony labyrinth of the fossil specimen were usually filled with matrix that is identical in density to those within the labyrinth cavity. As a result, automatic image processing cannot be used to isolate the endocast of the bony labyrinth from the surrounding matrix. Image processing, therefore, relied on manual tracing and reslicing using ImageJ and VGStudio Max 1.1 software. To ensure the accuracy of identified anatomical structures, image tracing and segmentation were carried out repeatedly, not only in the original x–y plane, but also in the resliced z–x and y–z planes.

Following manual image segmentation, image data sets of particular anatomical structures were imported into VGStudio Max 1.1 for 3D visualization. Volume rendering techniques were used for creating 3D images from the CT data.

Because the skull of *Chilecebus carrascoensis* is slightly distorted (a preservational artifact), the left and right bony labyrinths are not symmetrically positioned in the plane parallel to the palate (Fig. 1a). Bilateral symmetry therefore was restored during 3D visualization using the occipital condyles, foramen magnum, and posterior edges of the maxillae as reference points. An average of 7.7° offset relative to the coronal plane was required to reconstruct symmetry (Fig. 1b). Inferred from the shape of the tooth rows, occipital condyles, and the foramen magnum, there appears to be almost no distortion in other planes. The following measurements (Table 1) were taken from the restored reconstruction.

Measurement

We measured linear dimensions and orientations as defined by Spoor and Zonneveld (1995, 1998), derived from the 3D visualization of the CT data composited in VGStudio Max 1.1. Dimensions include the height and width of the three semicircular canals, as well as the basal turn of the cochlea. Proportions and shape indices of the semicircular canals were calculated based on linear measurements. Orientation angles were determined with reference lines added to the 3D visualizations; projections of these reference lines on transverse or sagittal planes were saved as separate images. These images then served as the basis for measuring angles using ImageJ software. To measure the planar orientation of the semicircular canals, we rotated the bony labyrinth to a position in which the projection of the central path of the semicircular canal can be fitted to a line, as much as possible. The central path of each canal is extracted by skeletonizing the separated images, using ImageJ and VGStudio Max 1.1. The common crus was included in the measure of planarity of the anterior and posterior semicircular canals.

The transverse plane is here defined as the one intersecting the nasion and both poria (Fig. 1c), known also as the nasion-biauricular plane (Clauser, 1980). This plane roughly parallels the lateral semicircular canal and is perpendicular to the anterior and posterior semicircular canals (Zonneveld, 1987; Spoor and Zonneveld, 1995, 1998). This reference frame allows direct comparison of our measurements of *Chilecebus carrascoensis* to data published by Spoor and Zonneveld (1998). It is important to note that this reference frame differs from the Horsley–Clark coordinate system, frequently used in vestibular studies (Blanks et al., 1972, 1975a,b, 1985; Curthoys et al., 1977). The Horsley–Clark transverse plane passes through the centers of the two external auditory meati and the infraorbital margins.

We present measurements (Table 1) of the left and right sides of paired features because of the potential variation caused by natural asymmetries in living organisms and the potential for preservational distortions in fossils (although as noted above, distortions in this specimen appear to be limited to a plane parallel to the palate). To increase accuracy, all measurements were repeated at least 5 times and averaged.

Statistical analyses

The radii of the semicircular canals have strong allometric relationships with body mass (Jones and Spells, 1963; Spoor and Zonneveld, 1998; Spoor et al., 2002, 2007). To eliminate the effect of body size and examine variation in the relative size of semicircular canals, semicircular canal radius was corrected for body mass (BM) by dividing the observed SCR (an average of the radii of the anterior, posterior, and lateral canals) with the predicted SCR size for a given BM, using the linear regression of *ln*SCR against *ln*BM for all primates (Fig. 4). The best available body mass estimate (583 g) for *Chilecebus carrascoensis* is from Sears et al. (2008).

Linear dimensions, proportions, orientation, and torsion angles taken from the same organ are not statistically independent, thus complicated correlations must exist among these variables. We used Principal Component Analysis (PCA) to further explore these correlations and the implications of the data published by Spoor and Zonneveld (1998), as well as in our new analyses of the bony labyrinth of *Chilecebus carrascoensis*. A matrix including 33 statistically correlated variables for 23 taxa was transformed via PCA into an orthogonal matrix with the same dimensions, from which rescaled Euclidean distances between the taxa were then calculated. The rescaled Euclidean distances can reveal similarities/dissimilarities among the sampled primates more effectively than raw linear dimensions, proportions, orientation, and torsion angles of the bony labyrinth. To better understand the correlations among variables, a Factor Analysis (FA) with Kaiser Varimax Rotation also was performed. All variables were standardized prior to undertaking PCA and FA, and the few missing data entries were replaced with means. All statistical analyses were performed using Aabel 2.4 software.

Results

Cochlea

The cochlea of *Chilecebus carrascoensis* is low and conical in form (Fig. 2). The left cochlea shows 2.5 spiral turns. The right cochlea is slightly deformed, probably as the result of a small crack, but 2.5 turns are still visible, although the second spiral turn of the cochlea does not overlap the first turn, leaving a significant gap between them. The modiolus of the cochlea is low and the entire cochlea resembles a very flat snail. In this respect it is very reminiscent of the cochlea in other anthropoids. Within primates, the second turn of the cochlea of some strepsirrhine taxa, such as *Nycticebus coucang* and *Lemur catta*, is relatively large and has a larger overlap covering the basal turn (Takahashi, 1976). As a result, the cochleae appear more conical than the cochleae of anthropoids—this may be a diagnostic difference between the two groups, but more species should be examined to clarify the distinction.

Recent statistical analyses have shown that cochlea size and body mass have a significant negative allometric relationship in

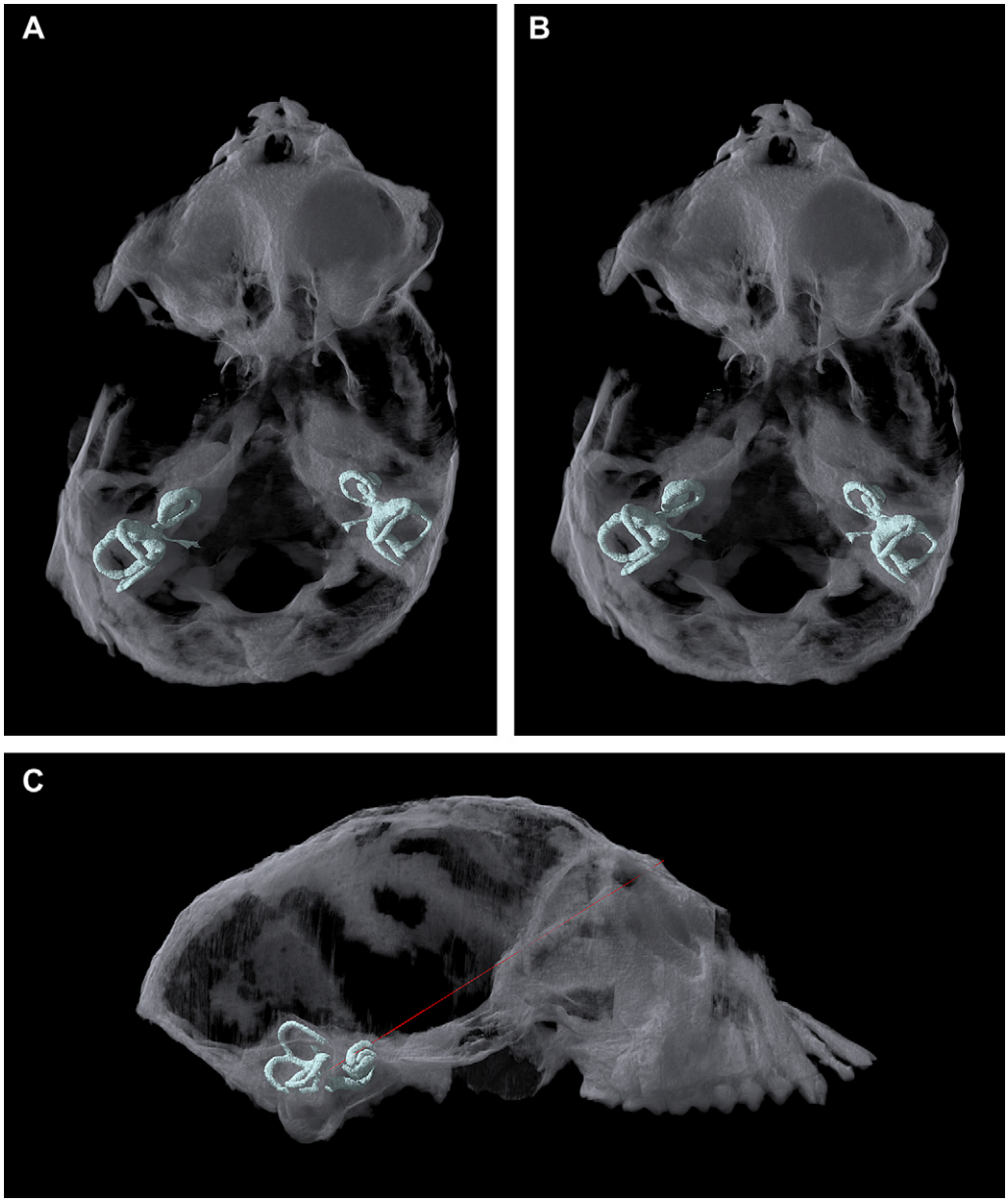

Fig. 1. Composite CT 3D visualization of the holotype skull of *Chilecebus carrascoensis*. To show the position of the bony labyrinths, the rest of the skull is set to transparent in this image. A) Dorsal view, unrestored, with the skull roof removed; B) dorsal view, restored with 7.7° offset, skull roof removed; C) lateral view, restored with 7.7° offset, red line indicates the nasion–biauricular plane.

mammals and that the relative size of the cochlea in primates falls within the range of variation observed in other mammals (Spoor et al., 2002). When the allometric relationship with body mass is taken into account, the cochlear radius (average of the two sides) of *Chilecebus carrascoensis* is similar to that in extant primates, most closely approximating the value for *Saimiri sciureus*. As in some other primates, the basal turn of the cochlea of *Chilecebus carrascoensis* is relatively taller dorsoventrally (height) than it is wide anteroposteriorly. The height/width ratio (percentage) varies greatly among extant primates. Nevertheless, the cochlea of *Chilecebus carrascoensis* is much rounder than in all other primates in which this feature has been examined.

The orientation of the cochlea can be efficiently described by the angular offset between the plane of its basal turn and the sagittal or transverse planes of the skull, as well as between the plane of the basal turn and the semicircular canals (Table 1). In dorsal view, the angles relative to the two vertical semicircular canals are measured relative to a line through the greatest width of the cochlea in the transverse plane (COt) and a line bisecting the anteroposteriorly opening angle between the arc orientations of the two vertical semicircular canals in the transverse plane (VSC). This angle, known for many living primates, can be translated into the angle between COt and the sagittal line in transverse plan (SG). In lateral view, the angle between the line across the maximal height of the basal turn (COs) and the line across the greatest width of the lateral semicircular canal (LSCm) is also measured. Because the COt and COs can represent the orientations of the cochlea in transverse and sagittal planes, respectively, and because the LSCm is very close to the horizontal plane when the nasion–biauricular plane is defined as the transverse plane, the COt $<$ SG and COs $<$ LSCm angles clearly define the geometric orientation of the cochlea in the skull. These two angles in *Chilecebus carrascoensis* fall well within the

Table 1
Linear dimension and orientations of the bony labyrinth of *Chilecebus carrascoensis*

Linear dimensions (mm) and orientations (degree)	Code	Right	Left	Mean
Height of the anterior semicircular canal	ASCh	2.94	2.93	2.93
Width of the anterior semicircular canal	ASCw	3.26	3.55	3.41
Radius of curvature of the anterior semicircular canal	ASCR	1.55	1.62	1.58
Height/width ratio of the anterior semicircular canal	ASCh/w	90.2	82.4	86.3
Height of the posterior semicircular canal (maximum AP diameter)	PSCh	3.12	3.18	3.15
Width of the posterior semicircular canal (perpendicular to height)	PSCw	2.69	2.69	2.69
Radius of curvature of the posterior semicircular canal	PSCR	1.45	1.47	1.46
Height/width ratio of the posterior semicircular canal	PSCh/w	115.9	118.1	117.0
Height of the lateral semicircular canal	LSCh	3.03	3.32	3.17
Width of the lateral semicircular canal	LSCw	2.80	2.89	2.85
Radius of curvature of the lateral semicircular canal	LSCR	1.46	1.55	1.50
Height/width ratio of the lateral semicircular canal	LSCh/w	108.1	114.9	111.5
Relative radius of the anterior semicircular canal (as a percent of the three radii)	ASC%	34.7	34.9	34.8
Relative radius of the posterior semicircular canal (as a percent of the three radii)	PSC%	32.6	31.6	32.1
Relative radius of the lateral semicircular canal (as a percent of the three radii)	LSC%	32.7	33.5	33.1
ASC-R index, observed ASCR/predicted SCR for a given BM from the linear regression of *ln*SCR against *ln*BM.	Index ASC	0.89	0.93	0.91
PSC-R index, observed PSCR/predicted SCR for a given BM from the linear regression of *ln*SCR against *ln*BM.	Index PSC	0.84	0.85	0.84
LSC-R index, observed LSCR/predicted SCR for a given BM from the linear regression of *ln*SCR against *ln*BM.	Index LSC	0.84	0.89	0.87
Maximum diameter of the ampulla of the anterior semicircular canal		1.32	1.25	1.29
Length of the ampulla of the anterior semicircular canal		1.80	1.64	1.72
Maximum diameter of the ampulla of the posterior semicircular canal		1.37	1.25	1.31
Length of the ampulla of the posterior semicircular canal		1.72	1.65	1.69
Maximum diameter of the ampulla of the lateral semicircular canal		1.20	1.22	1.21
Length of the ampulla of the lateral semicircular canal		1.58	1.68	1.63
Diameter of the tube of the anterior semicircular canal, at its vertex		0.42	0.42	0.42
Diameter of the tube of the posterior semicircular canal, at its vertex		0.43	0.41	0.42
Diameter of the tube of the lateral semicircular canal, at its vertex		0.42	0.45	0.43
Maximum external length of the common crus		2.58	2.15	2.36
Sagittal labyrinth index	SLI	33.2	32.0	32.6
Torsion of the anterior semicircular canal	ASCtor	18.7	1.5	10.1
Torsion of the posterior semicircular canal	PSCtor	−2.8	−8.3	−5.6
Torsion of the lateral semicircular canal	LSCtor	9.4	−1.9	3.7
Angle between the arc of the anterior semicircular canal, at its greatest width in the transverse plane, and the sagittal line	ASCm < SG	34.5	32.3	33.4
Angle between the arc of the posterior semicircular canal, at its greatest width in the transverse plane, and the sagittal line	PSCm < SG	140.8	127.9	134.4
Sum of ASCm < SG and PSCm < SG	CL VSC<	175.3	160.2	167.8
Angle between the arc of the lateral semicircular canal, at its greatest width in the sagittal plane, and the line connecting nasion and basion	LSCm < ba-na	1.5	−8.5	−3.5
Angle between the arc of the lateral semicircular canal, at its greatest width in the sagittal plane, and the line connecting the foramen caecum and the sella turcica	LSCm < s-fc	7.8	−1.8	3.0
Angle between the arc of the lateral semicircular canal, at its greatest width in the sagittal plane, and the line connecting the sella turcica and basion	LSCm < ba-s	2.3	−7.3	−2.5
Angle between the arc of the lateral semicircular canal, at its greatest width in the sagittal plane, and the line connecting basion and opisthion	LSCm < o-ba	−42.4	−54.1	−48.2
Angle between the arc of the lateral semicircular canal, at its greatest width in the sagittal plane, and the reference line representing the sagittal orientation of the posterior petrosal surface at the level of the common crus	LSCm < PPp	60.1	47.7	53.9
Angle between the arc of the anterior semicircular canal, at its greatest width in the transverse plane, and the arc of the posterior semicircular canal, at its greatest width in the transverse plane	ASCm < PSCm	106.6	96.1	101.4
Angle between an axis running through the greatest height of the lateral semicircular in the transverse plane and the reference line bisecting the anteroposteriorly opening angle formed by the arc orientations of the two vertical semicircular canals in the transverse plane	LSCt < VSC	101.0	109.4	105.2
Angle between the common crus in the sagittal plane and the arc of the lateral semicircular canal at its greatest width in the sagittal plane	CCR < LSCm	123.0	107.8	115.4
Angle between the line connecting the centers of the ampullae of the anterior and posterior semicircular canals in the sagittal plane and the arc of the lateral semicircular canal at its greatest width in the sagittal plane	APA < LSCm	36.8	26.8	31.8
Angle between a line through the greatest width of the cochlea in the transverse plane and the reference line bisecting the anteroposteriorly opening angle formed by the arc orientations of the two vertical semicircular canals in the transverse plane	COt < VSC	129.7	130.3	130.0
Angle between the vestibulocochlear line in the sagittal plane and the arc of the lateral semicircular canal at its greatest width in the sagittal plane	VC < LSCm	158.2	149.0	153.6
Angle between a line running through the greatest height of the cochea in the sagittal plane and the arc of the lateral semicircular canal at its greatest width in the sagittal plane	COs < LSCm	42.9	48.5	45.7
Planar angle between the anterior and posterior semicircular canals		94.3	87.7	91.0
Planar angle between the anterior and lateral semicircular canals		93.1	91.9	92.5
Planar angle between the posterior and lateral semicircular canals		105.7	91.7	98.7
Planar angle between the left and right lateral semicircular canals (ventral angle)				168.7
Planar angle between the right anterior and left posterior semicircular canals				172.6
Planar angle between the left anterior and right posterior semicircular canals				172.9

Table 1 (*continued*)

Linear dimensions (mm) and orientations (degree)	Code	Right	Left	Mean
Angle between the sagittal line and the reference line representing the transverse orientation of the posterior petrosal surface at the level of the lateral semicircular canal	PPip < SG	140.2	136.0	138.1
Angle between the line from the foramen caecum to the sella turcica in the sagittal plane and the reference line representing the sagittal orientation of the posterior petrosal surface at the level of the common crus	PPp < s-fc	128.8	130.3	129.5
Angle between the line from the sella turcica to the basion in sagittal plane and the line from the foramen caecum to the sella turcica	ba-s < s-fc			185.9
Angle between the line from basion to opisthion in the sagittal plane, and the line from the foramen caecum to the sella turcica	o-ba < s-fc			51.7
Height of the basal turn of the cochlea	COh	2.82	2.93	2.88
Width of the basal turn of the cochlea	COw	2.79	2.85	2.82
Radius of curvature of the basal turn of the cochlea	COR	1.40	1.45	1.42
Height/width ratio of the basal turn of the cochlea	COh/w	100.8	103.0	101.9
Angle between a line through the greatest width of the cochlea in the transverse plane and the sagittal line	COt < SG	127.3	120.1	123.7
Modiolar height		1.65	1.66	1.66
Cochlear spiral turn number		2.50	2.50	2.50
Planar orientation (angle) of the basal turn relative to the sagittal plane		121.8	119.3	120.5
Extension of the vestibular aqueduct		3.24	3.24	3.24

variation measured in other primates (Fig. 3). However, no clear relationship between cochlear orientation and phylogenetic affinity or body mass is observed in Figure 3.

Vestibule

The vestibular part of the bony labyrinth of *Chilecebus carrascoensis* is reasonably well preserved on the right side. The lateral wall of the left bony vestibule is slightly damaged (Fig. 2). The posterior part of the cochlea is fairly straight; after extending posterodorsally for a very short distance it makes a small turn to join the vestibule. This straight part of the cochlea on the right side seems to have a tiny offset, probably due to a small crack. In lateral view the straight segment of the cochlea approaches the vestibular part in a manner similar to that in some modern anthropoids, but differing from the arrangement in the strepsirrhines *Lemur* and *Nycticebus*, wherein the straight portion of the cochlea is more dorsally directed (see Takahashi, 1976).

In dorsal view, the posterior part of the bony vestibule bears a prominent, anteromedially facing bulge on the dorsal side, sitting immediately anterior of the two ampullae of the anterior and lateral semicircular canals. This bulge forms a circular depression within the bony cavity, known as the spherical recess, enclosing the anterodorsal part of the utricular vestibular sac. The vestibule is relatively smooth and pillar-like from the medial side of the spherical recess to the dorsomedial wall of the vestibule. The common crus of the two vertical semicircular canals connect to the dorsal and medial part of the vestibule.

Immediately medioventral to the common crus, the large ampulla of the posterior semicircular canal joins the vestibule. The posterior end of the lateral semicircular joins the vestibule posterior of and slightly dorsal to the conjunction of the common crus and the ampulla of the posterior semicircular canal. A thin and curved canal, identified as the vestibular aqueduct, originates from the medioventral aspect of the vestibule anterior and ventral to the ampulla of the posterior semicircular. This canal runs nearly horizontally and opens posterior to the internal acoustic meatus. The vestibular aqueduct transmits a small vein and contains the endolymphatic duct, which terminates in the endolymphatic sac between the layers of dura mater.

The wall of the posterior part of the vestibule is relatively flat, joining the ampullae of the lateral and posterior semicircular canals. On the ventral side of the vestibule there is a short funnel-shaped process, the endocast of the round window, lying just posterior to the vestibular aqueduct. An oval projection lies ventral to the ampulla of the lateral semicircular canal, on the lateral wall of the spherical recess. Its long axis is oriented roughly anteroposteriorly. This projection is identified as the endocast of the oval window.

Semicircular canals

Semicircular canal sizes correlate allometrically with body mass in extant vertebrates (Jones and Spells, 1963; Spoor and Zonneveld, 1998; Spoor et al., 2007; Walker et al., 2008). The relative size of the semicircular canals in primates is comparable to those in other mammals, except cetaceans, in which the semicircular canals are unusually small (Fig. 4). A regression line for primates alone lies slightly above the regression for mammals generally, indicating that the radii of the semicircular canals in primates are slightly larger than expected for mammals of their size. However, this slight difference probably is not meaningful, as the primate distribution substantially overlaps that for other non-cetacean mammals (Fig. 4).

When plotted against body mass, the average semicircular canal size of *Chilecebus carrascoensis* is smaller than the average of extant primates; nonetheless, it falls within the range observed in extant primates (Fig. 4). After being corrected for body mass, the three semicircular canals, particularly the anterior and posterior, have a roughly linear relationship of the relative semicircular sizes (or indices, Fig. 5). Following Spoor et al.'s (2007) assessment of locomotor agility, agile primates (across taxonomic subgroups) tend to have larger semicircular canals, particularly the lateral one, than do less agile species (Fig. 5), although broad overlaps exist among different agility categories. The semicircular canal indices of *Chilecebus carrascoensis* fit well within the variation associated with this general across–primate correlation (Fig. 5). However, no phylogenetic or agility category signal can be detected for this and other taxa with similar relative semicircular canal sizes. A broad array of extant taxa, such as *Saguinus oedipus*, *Callithrix jacchus*, *Microcebus rufus*, *Microcebus murinus*, *Cheirogaleus major*, and *Gorilla gorilla*, all have semicircular canal indices similar to those of *Chilecebus carrascoensis*.

The anterior semicircular canal of *Chilecebus carrascoensis* is slightly larger than the lateral and posterior canals, and the posterior semicircular canal is proportionally the smallest (Table 1). A range of living primates possess semicircular canal proportions similar to those of *Chilecebus carrascoensis*, including *Otolemur garnettii*, *Galago moholi*, *Hylobates molocha*, and *Cercocebus torquatus* (Fig. 6). No correlation between agility categories and

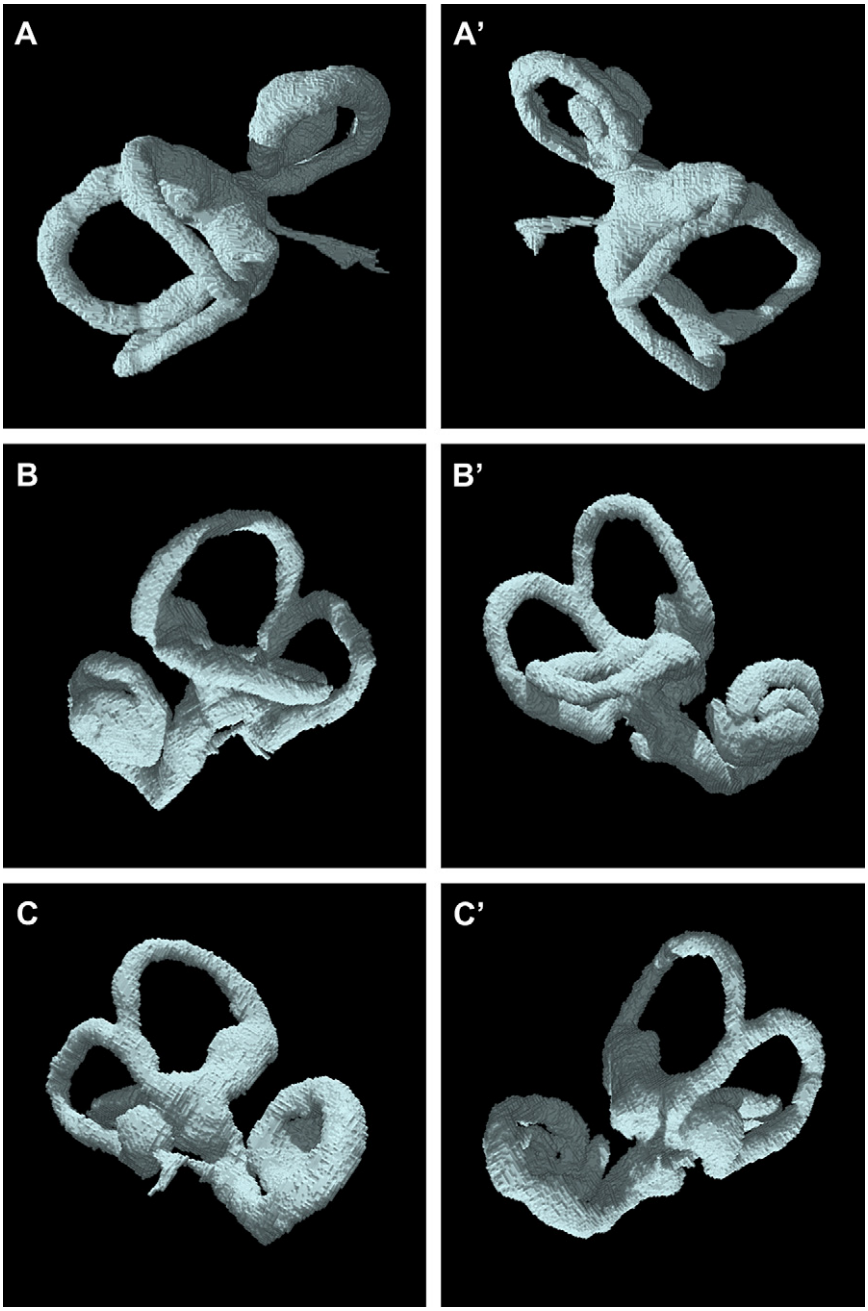

Fig. 2. 3D reconstructions of the bony labyrinths of *Chilecebus carrascoensis*. A) Left dorsal view, A′) right dorsal view; B) left lateral view B′) right lateral view; C) left medial view, C′) right medial view.

variation in the proportion of semicircular canals is detected in such a plot.

The size of the ampullae of *Chilecebus carrascoensis* falls within the range observed in the few other primates for which it has been reported (Takahashi, 1976). The size is close to the values for *Chilecebus jacchus* and *Saimiri sciureus*.

The semicircular canals of *Chilecebus carrascoensis* are not completely circular. The height/width ratio (percentage) of the anterior canal is similar to that of some catarrhines, such as *Macaca fascicularis*, *Papio ursinus*, and *Mandrillus sphinx*, but differs from all sampled platyrrhines (including *Cebus apella*, *Saimiri sciureus*, *Lagothrix lagothricha*, and *Alouatta seniculus*) wherein the anterior canal is taller than wide (Fig. 7a). The posterior semicircular canal of *Chilecebus carrascoensis* is much more posteriorly extended than in other platyrrhines, marginally falling within the range of variation in catarrhines (Fig. 7a). The lateral semicircular canal in *Chilecebus carrascoensis* is also relatively high. The height/width ratio is higher than in all other sampled primates (Fig. 7a).

The degree of planarity of the semicircular canals is quantified by various methods. Blanks et al. (1985) averaged the most extreme points above and below the best-fit plane for any given canal, whereas Spoor and Zonneveld (1995, 1998) measured the torsion angle of each canal. The anterior and lateral semicircular canals of *Chilecebus carrascoensis* show a degree of torsion or non-planarity, whereas the posterior canals are fairly planar. The right lateral canal shows more anterior–posterior torsion than the left. Both anterior canals show the characteristic anterior bending seen in other anthropoids. Following the method of Spoor and Zonneveld (1995,

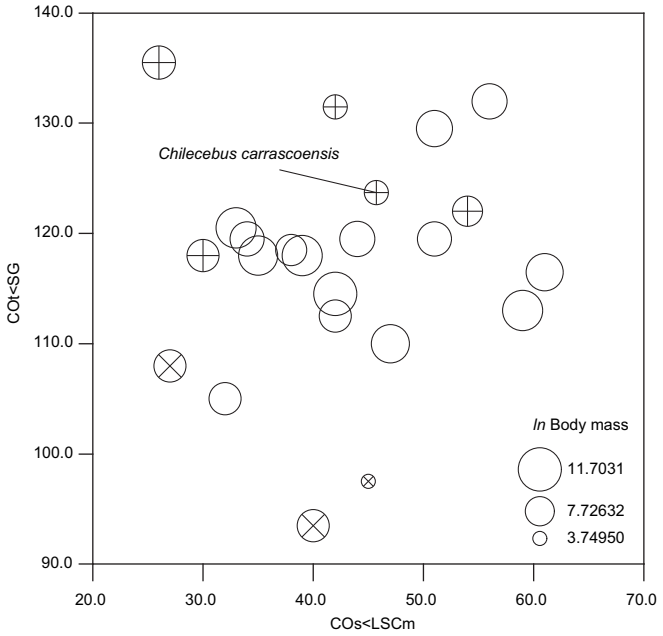

Fig. 3. Bivariate plot of COt < SG and COs < LSCm angles, indicating the orientation of the cochlea of *Chilecebus carrascoensis* and other primates. Circles with "X" = strepsirrhines, circles with " + " = platyrrhines, empty circles = catarrhines. The radii of the circles reflect the body mass for each taxon.

1998), the average of the two sides lies within the range of other primates (Fig. 7b).

The planar orientation of the ipsilateral semicircular canals departs slightly from orthogonal in *Chilecebus carrascoensis* (Table 1). The pairs of synergistically acting canals (Blanks et al., 1972, 1985; Graf, 1988) are the right and left lateral, right anterior and left posterior, and left anterior and right posterior semicircular

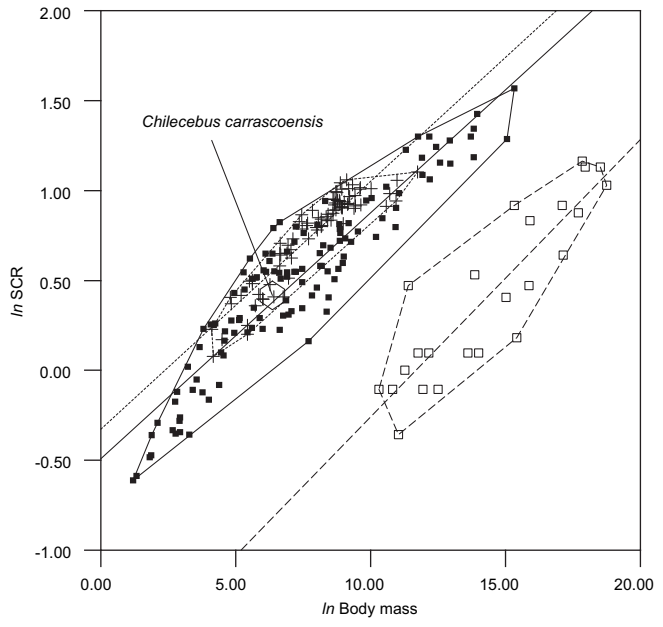

Fig. 4. Allometric relationships between body mass and the average radii of the three semicircular canals (SCR). Crosses and dot line = extant primates ($y = 0.14x - 0.33$, $r^2 = 0.86$), squares and dashed line = extant cetaceans ($y = 0.15x - 1.80$, $r^2 = 0.80$), black block and solid line = other extant mammals ($y = 0.14x - 0.49$, $r^2 = 0.87$). Data, except for *Chilecebus carrascoensis*, are from Spoor et al. (2002, 2007). Body masses of extant primates are from Smith and Jungers (1997).

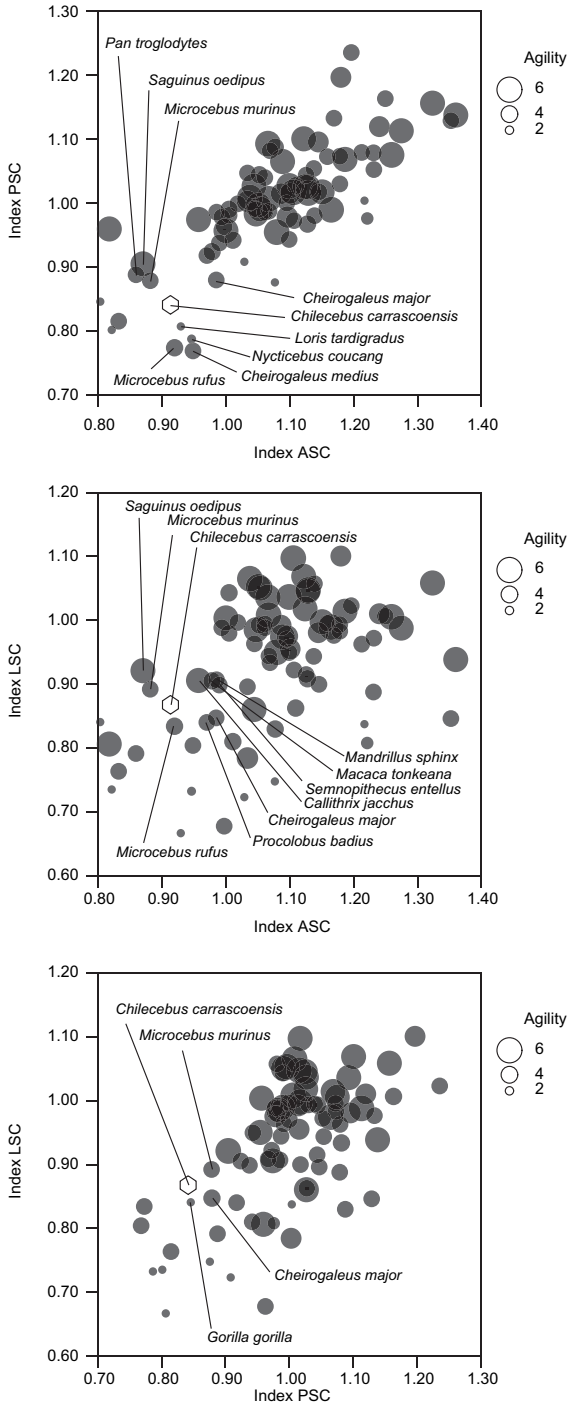

Fig. 5. Size indices of the anterior (ASC), posterior (PSC), and lateral (LSC) semicircular canals among primates. A) PSC against ASC, B) LSC against ASC, C) LSC against PSC. Indices are the observed size divided by predicted size. Data, except for *Chilecebus carrascoensis*, are from Spoor et al. (2007). Dot size indicates level of agility, as defined by Spoor et al. (2007). Individual dot pattern is set as semitransparent; overlapping dots are darker; in cases of multiple overlaps, points appear black.

canals. In *Chilecebus carrascoensis*, the paired contralateral horizontals form an angle about 11° off parallel, while the two synergistically acting vertical canal pairs are oriented close to parallel.

Spoor and Zonneveld (1998) reported the angle between the arcs at the greatest width of the anterior and posterior semicircular canals on the transverse plane (ASCm < PSCm) in 22 living primates. Because of the difference in definition, the angles

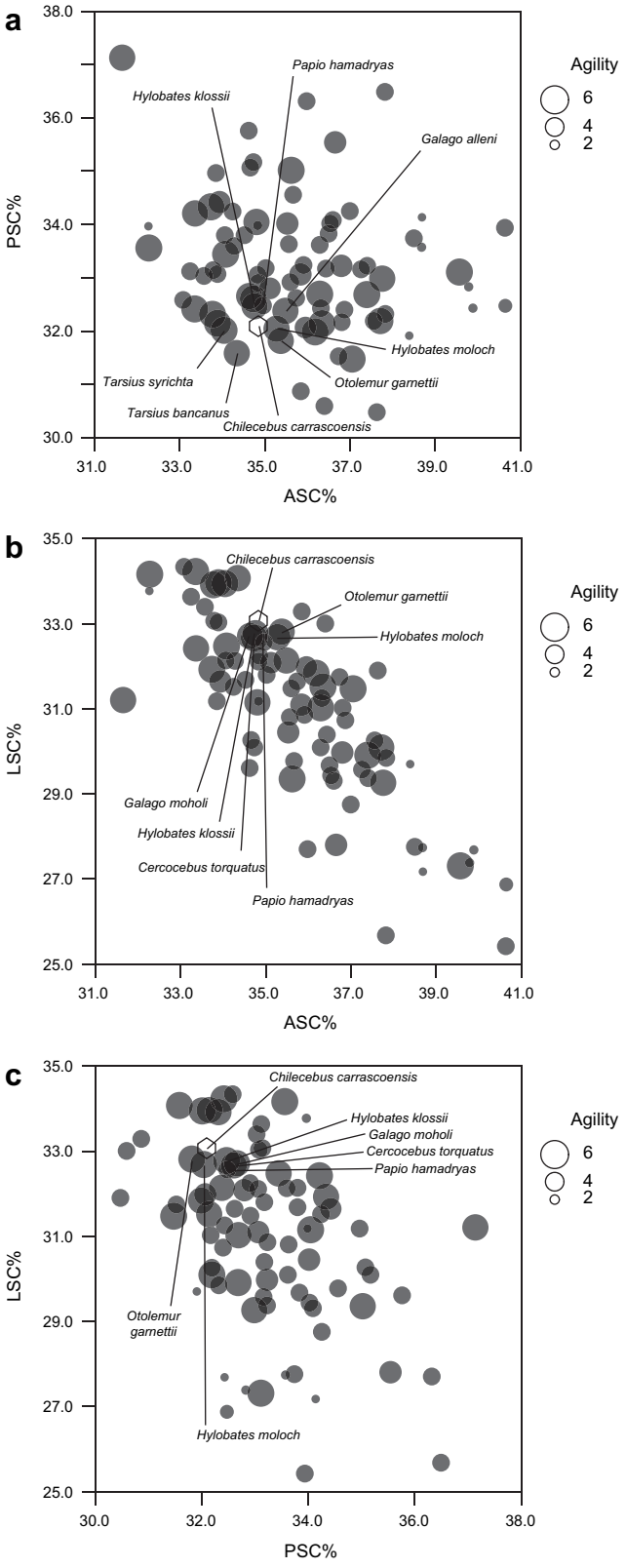

Fig. 6. Radius of the anterior (ASC), posterior (PSC), and lateral (LSC) semicircular canals as a fraction of the sum of all three radii. A) PSC against ASC, B) LSC against ASC, C) LSC against PSC. Data, except for *Chilecebus carrascoensis*, are from Spoor et al. (2007). Dot size indicates level of agility as defined by Spoor et al. (2007). Individual dot pattern is set as semitransparent; overlapping dots are darker; in cases of multiple overlaps, points appear black.

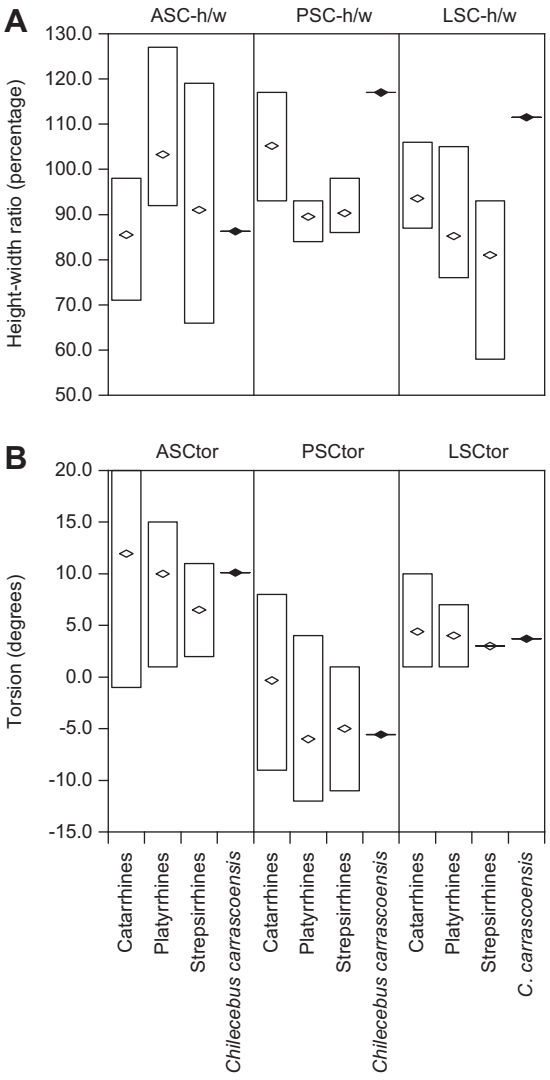

Fig. 7. The shape of the semicircular canals in selected primates. A) Height/width ratio (percentage), B) torsion. Bar indicates the range of values; rhombus indicates the mean. Data, except for *Chilecebus carrascoensis*, are from Spoor and Zonneveld (1998).

reported by Spoor and Zonneveld (1998) differ from the planar angle between the anterior and posterior semicircular canals, but their measures may covary with the planar angle. According to their data, in most primates the angle between the anterior and posterior semicircular canals is significantly >90°. Three strepsirrhines, *Propithecus diadema*, *Indri indri*, and *Microcebus rufus* have values approaching 90°, less than in all anthropoids. Platyrrhine and catarrhine anthropoids have an overlapping distribution spanning 101°–110°. In *Chilecebus carrascoensis*, the average of ASCm < PSCm angle is 101.4°, barely falling within the range of variation in living anthropoids (Fig. 8).

The sum of the angles of ASCm < SG and PSCm < SG (CL VSC<) can be seen as an approximation of the planar angles between the synergistically acting VSC pairs. The 22 taxa investigated in Spoor and Zonneveld (1998) shows a small departure from parallel (Fig. 8). As noted above, three sampled strepsirrhines, *Propithecus diadema*, *Indri indri*, and *Microcebus rufus*, differ from other primates in having relatively small ASCm < PSCm angles, but they overlap the range of the CL VSC< observed in anthropoids. *Lagothrix lagothricha* and *Alouatta seniculus* differ markedly from other primates, indicating that their synergistically acting VGC

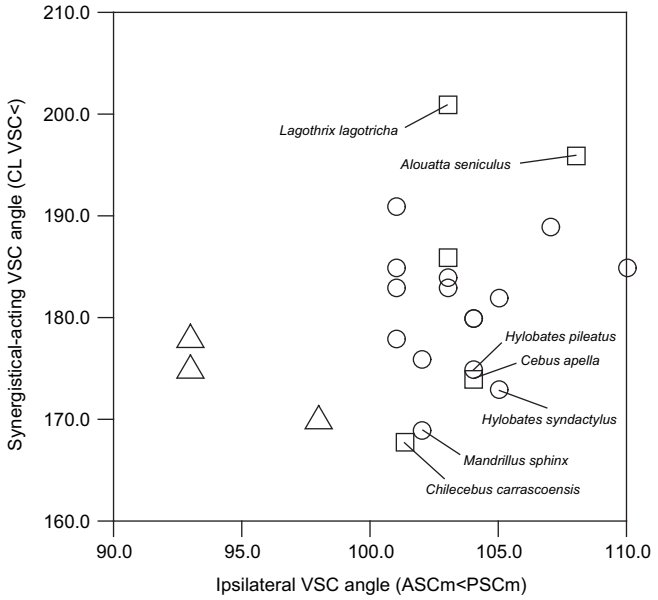

Fig. 8. Angles between ipsilateral vertical semicircular canals (ASCm < PSCm) and between paired synergistical acting VSC (CL VSC<). Triangle = strepsirrhines, circle = catarrhines, square = platyrrhines. Data, except *Chilecebus carrascoensis*, are from Spoor and Zonneveld (1998).

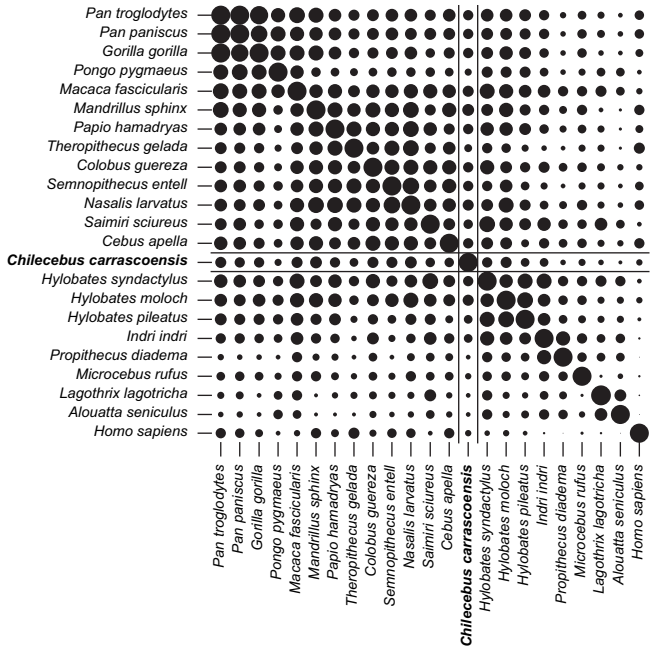

Fig. 9. Similarity matrix based on rescaled Euclidean distances. Dot radius reflects the degree of similarity, calculated as one minus the rescaled Euclidean distances. Raw data, except for *Chilecebus carrascoensis*, are from Spoor and Zonneveld (1998).

pair are much less parallel. The CL VSC< in *Chilecebus carrascoensis* is small, but it does not markedly deviate from that observed in other anthropoids (Fig. 8).

The angles between the arc of the lateral semicircular canal at its greatest width in the sagittal plane and the reference lines of the cranial floor (Table 1) reflect the variation of semicircular canal orientation relative to the shape of the cranial floor (Spoor and Zonneveld, 1998). *Chilecebus carrascoensis* is within the range of reported angles for extant primates.

Principal component analysis, rescaled Euclidean distances, and factor analysis

Using Principal Component Analysis (PCA), we extracted principal components for calculating rescaled Euclidean distances and then a similarity measure. The similarities, calculated as one minus the rescaled Euclidean distances, suggest that the modern primates investigated fall into several groups (Fig. 9). The four species of nonhuman great apes form one such grouping. Quadrupedal "monkeys," including macaques, baboons, mandrills, colobines, capuchin, and squirrel monkeys, form a large group with similar dimensions and orientation of the semicircular canals, but this resemblance does not seem to closely correspond to locomotor style or "agility." Some members of this group are generalized; for example, *Macaca fascicularis* and *Saimiri sciureus* share relatively strong similarities with most other primates. Not surprisingly, the three gibbons are very similar to each other. Despite their specialized locomotor pattern, however, they are similar to quadrupedal monkeys and nonhuman hominoids as well. *Propithecus diadema* is very distinct from other sampled primates except *Indri indri*, although *Propithecus diadema* seems even more specialized. *Lagothrix lagothricha* and *Alouatta seniculus* are highly idiosyncratic, clustering together, but apart from all other primates. Humans exhibit only low levels of similarity to chimpanzees and gorillas, as well as some quadrupedal monkeys. Presumably, the marked distinction between humans and all other primates reflects bipedality in humans. *Microcebus rufus* is another taxon that exhibits a low level of similarity to other primates; it joins only *Indri indri* and *Propithecus diadema* at a low similarity value. *Chilecebus carrascoensis* shows moderate levels of similarity to most other sampled primates. It marginally approaches the group including quadrupedal monkeys, but it is not closely similar to any extant taxa, reflecting a unique labyrinth morphology relative to all living primates for which such data are available.

The PCA exploration reveals that eigenvalues of the first nine principle components are greater than one. That is, these nine components account for more variance than does any single variable. The first three principle components account for more than 50% of the variation, and the first nine capture over 90% of the total variance (Table 2). The first principle component accounts for 29.7% of the total variance. The second and third components also have high eigenvalues, each accounting for about 14% of the variance. The remaining six components have relatively smaller eigenvalues, each accounting for less than 10% of the variance.

The Factor Analysis (FA) was used to extract these first nine principle components as FA factors. The loadings on the factors, with Kaiser Varimax Rotation applied, are shown in Table 3. The angles formed by the lateral semicircular canal relative to the reference lines of cranial floor, cochlea, common crus, and ampullae have their highest correlations with Factor 1. The sagittal labyrinth index and the torsion of the posterior semicircular canal also load principally on Factor 1. Factor 2 has three main loadings: the angle between the two vertical semicircular canals and both the angles of the cochlea relative to the sagittal plane and to the vertical semicircular canals. The loadings of the third factor mainly reflect the shape or angles of the cranial floor, with a high correlation also with the percentage of the radius of the posterior semicircular canal relative to the sum of the three radii. The percentages of the anterior and lateral semicircular canals and the height/width ratios of the two vertical semicircular canals are characteristic of Factor 4. The height/width ratio of the lateral semicircular canal singly loads on Factor 5. The

Table 2
Principle component analysis: eigenvalues and variance percentages explained by each principle component (PC) and cumulatively

	PC 1	PC 2	PC 3	PC 4	PC 5	PC 6	PC 7	PC 8	PC 9
Eigenvalues	9.79	4.59	4.54	2.89	2.15	1.94	1.75	1.26	1.18
Variance (%)	29.66	13.91	13.77	8.77	6.51	5.88	5.29	3.80	3.58
Variance (Cum. %)	29.66	43.57	57.34	66.11	72.61	78.49	83.79	87.59	91.17

indices of the three semicircular canals are the main loadings of Factor 6. Torsions of the anterior and lateral semicircular canals are not grouped with torsion of the posterior canal, but instead contribute most strongly to Factor 7. The angles of the vertical semicircular canals relative to the sagittal plane and the angle of contralateral vertical canals have their largest loadings on Factor 8. The angle between the lateral semicircular canal and the reference line for the vertical semicircular canals is most highly correlated with Factor 9.

Discussion

Cochlear morphology

The primate hearing apparatus is considered advanced in its ability to discriminate minute changes in amplitude and spectral composition of acoustic waveforms (Stebbins, 1978, 1980). Nevertheless, the gross morphology of inner ear structures differs little between primates and other mammals (Stebbins, 1978). The cochleae of *Chilecebus carrascoensis* differs from other anthropoids only by being a bit rounder (height/width ratio of the basal turn is closer to 100) than those of studied primates. This unique condition and the limited knowledge of the cochleae in most fossil primates makes it impossible to determine whether this shape is due to phylogeny (e.g., an autapomorphy for *Chilecebus carrascoensis*, or retention of a primitive platyrrhine or anthropoid condition) or functional specialization of this fossil taxon. No previous research suggests that cochlear roundness is related to hearing capability.

The number of cochlear spiral turns ranges from 1.5 to 4.5 turns in living mammals, and there is not a clear phylogenetic pattern (Gray, 1907, 1908a,b; Watt, 1917; de Burlet, 1934). West (1985) has suggested that the number of spiral turns in the cochlea is potentially correlated to the octave range of audible frequencies in ground dwelling mammals, independent of basilar membrane length. Other workers have suggested, however, that the number of spiral turns of the cochlea is less important in this function than the number of hair cells and unmedullated nerve fibers in the organ of Corti (Werner, 1960).

Primates show a similarly large range of variation: *Daubentonia madagascariensis* has only 1.5 turns, whereas *Cebus albifrons*, *Ateles belzebuth*, and *Papio papio* have as many as 3.25 turns (Werner, 1960). The number of spiral turns in *Chilecebus carrascoensis* (2.5) falls within the range of other primates, but is lower than in most anthropoids. Considering the large variation of the spiral turns among species, and sometimes even within a single species (Takahashi, 1976), it is unclear whether the fewer spiral turns in *Chilecebus carrascoensis* represents a primitive anthropoid or platyrrhine condition.

Table 3
Factor analysis: factor loadings for measured variables[a]

	Vmax factor 1	Vmax factor 2	Vmax factor 3	Vmax factor 4	Vmax factor 5	Vmax factor 6	Vmax factor 7	Vmax factor 8	Vmax factor 9
APA < LSCm	**−0.91**	−0.03	−0.31	0.04	0.10	0.03	0.07	0.03	−0.14
COs < LSCm	**−0.90**	0.07	−0.13	0.03	−0.15	−0.15	0.05	−0.23	−0.01
LSCm < s-fc	**−0.87**	−0.01	0.10	−0.10	0.21	0.25	−0.18	0.03	0.01
LSCm < PPp	**−0.82**	0.17	−0.13	0.21	0.12	−0.27	−0.17	−0.30	−0.09
SLI	**−0.74**	0.06	−0.35	−0.33	−0.28	−0.02	0.16	−0.03	−0.03
CCR < LSCm	**−0.70**	−0.09	−0.12	−0.03	−0.32	−0.01	−0.04	−0.14	0.49
VC < LSCm	**−0.62**	0.35	−0.21	−0.12	0.26	0.16	−0.09	−0.14	0.43
LSCm < ba-na	**−0.61**	0.05	−0.58	−0.35	0.00	−0.17	−0.16	0.09	−0.18
PSCtor	**0.54**	0.11	−0.28	−0.36	0.38	0.04	0.13	0.06	−0.34
PPp < s-fc	**0.51**	−0.22	0.23	−0.33	−0.03	0.49	0.12	0.40	0.14
ASCm < PSCm	0.04	**0.89**	−0.20	0.06	−0.10	0.00	0.35	−0.06	−0.01
COt < SG	−0.14	**0.84**	−0.07	0.04	0.22	−0.14	−0.19	0.34	0.03
COt < VSC	−0.24	**0.80**	−0.12	−0.04	0.29	−0.18	−0.28	−0.02	0.03
ba-s < s-fc	0.15	−0.06	**0.94**	0.05	0.06	0.15	0.02	0.01	0.10
o-ba < s-fc	0.10	−0.11	**0.90**	0.04	−0.09	0.24	−0.02	0.06	−0.12
LSCm < o-ba	−0.49	0.09	**−0.78**	−0.09	0.19	−0.11	−0.07	−0.04	0.12
LSCm < ba-s	−0.55	0.05	**−0.78**	−0.11	0.05	−0.01	−0.09	0.00	−0.08
PSC%	0.00	0.11	**−0.70**	0.43	0.03	−0.19	0.09	−0.29	−0.22
PPip < SG	−0.11	−0.21	**0.62**	0.12	−0.06	0.34	−0.15	0.39	−0.24
LSC%	−0.04	−0.08	0.12	**−0.96**	0.08	−0.05	0.02	−0.18	−0.03
ASC%	0.04	0.01	0.33	**0.77**	−0.10	0.18	−0.08	0.39	0.19
ASCh/w	−0.15	0.10	0.32	**0.57**	0.41	0.34	−0.06	0.35	−0.14
PSCh/w	−0.24	0.07	−0.38	**−0.39**	0.32	0.10	0.26	−0.34	0.34
LSCh/w	0.01	0.17	−0.14	−0.07	**0.88**	0.11	0.05	−0.06	0.10
Index PSC	0.02	−0.08	0.13	0.34	0.10	**0.89**	0.06	−0.05	−0.11
Index LSC	−0.02	−0.14	0.36	−0.42	0.12	**0.78**	0.04	−0.06	−0.03
Index ASC	0.05	−0.09	0.41	0.43	0.04	**0.75**	−0.02	0.20	0.04
LSCtor	0.16	0.06	0.09	−0.14	0.03	0.17	**0.86**	0.05	0.17
ASCtor	−0.11	−0.12	−0.15	0.11	0.11	−0.55	**0.68**	0.05	−0.21
ASCm < SG	0.18	−0.05	0.13	0.20	0.02	−0.01	−0.05	**0.91**	−0.01
CL VSC<	0.16	0.39	0.05	0.20	−0.03	0.01	0.11	**0.85**	−0.01
PSCm < SG	0.13	0.66	−0.02	0.17	−0.07	0.02	0.21	**0.66**	−0.01
LSCt < VSC	−0.24	−0.04	−0.15	−0.41	−0.35	0.20	−0.26	−0.09	**−0.66**

[a] Bold values indicate the largest absolute value of loadings on factors, for each measured variable.

Semicircular canal dimensions and activity patterns

The size of the ampulla, the radii of curvature, and its cross-section are the main controls of the dynamic response of the semicircular canals to head rotation (Steinhausen, 1933; Jones and Spells, 1963; Ten Kate et al., 1970; Howland and Masci, 1973; Hullar, 2006; Yang and Hullar, 2007). Biophysical modeling theory suggests that the sensitivity of the semicircular canals can be predicted from these three parameters (Steinhausen, 1933; Jones and Spells, 1963; Ten Kate et al., 1970; Hullar, 2006; Yang and Hullar, 2007). However, recent experimental studies indicate an inconsistent correlation between afferent sensitivity and dimensions of the semicircular canals (Hullar, 2006; Yang and Hullar, 2007).

The potential correlation between the dimensions of the semicircular canals, afferent sensitivity, and locomotor pattern has been interpreted in various ways. Jones and Spells' (1963) classic hypothesis suggested that animals typified by slow head movements have larger, more sensitive semicircular canals tuned to low velocities, whereas animals with fast head motions have smaller, less sensitive semicircular canals, thereby avoiding excitatory or inhibitory saturation of the system in high velocity movements. As a supporting example, the semicircular canals of subterranean rodents and moles are relatively large, presumably in response to the increased need for orientation cues from the vestibular organ (Lindenlaub et al., 1995; McVean, 1999). In the gigantic sauropod dinosaur, *Brachiosaurus brancai*, the anterior semicircular canal is significantly larger than the allometric relationship would predict, a pattern interpreted as an adaptation for slow movements of the head (Clarke, 2005). The opposite hypothesis suggests that agile, rapidly moving animals should have semicircular canals with larger curvatures. In birds, aspects of the semicircular canals have been found to vary with mode of life, capable fliers being characterized by larger canals (Hadžiselimović and Savković, 1964). A similar anomaly is seen among primates: the semicircular canals of the agile, leaping *Tarsius bancanus* are large compared to the slow climbing lorises *Loris tardigradus* and *Nycticebus coucang* (Matano et al., 1985, 1986).

Among extant primates large semicircular canals were suggested to correlate with high "agility" (Spoor et al., 2007). By using the predictive equations for primates provided by Silcox et al. (2009), the agility of *Chilecebus carrascoensis* can be estimated as 3.58 based on the SCR, 3.69 based on the ASCR, 3.60 based on the PSCR, or 4.03 based on the LSCR. These estimated values indicate moderate agility compared with the variation (2–6) observed in extant primates. However, there may be substantial uncertainty in this inference given that potential arbitrariness could be introduced by binned agility cataloging and the observation that taxa with similar semicircular canal size indices have been assigned to widely different agility catalogs in previous studies (also Fig. 5).

Proportions of the semicircular canals vary considerably among modern primates and may correlate with agility or other factors (Spoor et al., 1994, 1996, 2007; Spoor and Zonneveld, 1998; Walker et al., 2008). Because the anterior semicircular canal is larger than the posterior and lateral canals in many species, relative anterior canal size has been associated with particular locomotor patterns (Graf and Vidal, 1996; Spoor and Zonneveld, 1998; Hullar, 2006). However, recently overall size of the anterior canal and the width of the posterior canal have been shown to correlate more strongly with subarcuate fossa size than with agility (Jeffery et al., 2008). Wider taxonomic sampling reveals that enlargement of the anterior semicircular canal is not clearly correlated with any single locomotor style. For example, primates with very different agility catalog assignments and locomotor patterns, such as *Ateles*, *Alouatta*, *Daubentonia*, *Arctocebus*, *Nycticebus*, and *Perodicticus*, all have proportionally very large anterior semicircular canals (Spoor and Zonneveld, 1998; Spoor et al., 2007).

A plot (Fig. 6) of proportions of each semicircular canal, together with agility catalog assignments, fails to reveal a pattern that could be used for confidently predicting the agility of *Chilecebus carrascoensis*. Because of these uncertainties, we can only conclude that *Chilecebus carrascoensis* may have been moderately agile, probably not as agile as other small-bodied extant platyrrhines such as *Leontopithecus rosalia*, *Saguinus oedipus*, and *Callithrix jacchus*. Considering its generalized semicircular canal proportions, which are typical of most primates (Fig. 6), it is reasonable to conclude that *Chilecebus carrascoensis* probably was not a suspensory acrobat or a slow climber.

Shape and orientation of the semicircular canals

The shorter-than-wide anterior semicircular canal and elongated posterior canal in *Chilecebus carrascoensis* differ from all sampled living platyrrhines, but resemble some catarrhines (Fig. 7a). This may suggest that this shape feature is either primitive for anthropoids or convergent between *Chilecebus carrascoensis* and those catarrhines. Previous research did not reveal significant differences in height/width ratio of the lateral semicircular canals among extant primates. The relatively higher lateral semicircular canal in *Chilecebus carrascoensis* than in any other sampled primate suggests an autapomorphic condition in this taxon.

In primates, the anterior semicircular canal generally shows the greatest degree of non-planarity. Its dorsal edge is bent significantly forward in *Saimiri*, *Callitrix*, *Cercopithecus*, *Hylobates*, several species of *Macaca*, and human, but not in *Lemur catta* and *Nycticebus coucang* (Takahashi, 1976; Blanks et al., 1985). Spoor and Zonneveld (1998) also showed that in primates the anterior semicircular canals tend to have a larger torsion angle than the posterior and lateral canals (Fig. 7b). The anterior semicircular canal of *Chilecebus carrascoensis* has a larger torsion angle than the posterior and the lateral canals as in extant primates and the anterior bending typically seen in extant anthropoids. Thus, larger torsion may be primitive for primates and anterior bending may be a feature of all anthropoids. However, greater taxonomic sampling will be required to assess the relative influences (if any) of phylogeny or locomotor function on these shape features.

The angles between the ipsilateral semicircular canals and the synergistically acting pairs of semicircular canals represent main orientation features. The ipsilateral canals are perpendicular to one another proximally, but otherwise are not completely orthogonal (Graf, 1988). Departures from mutual orthogonality are significant in many species, including toadfish (Ghanem et al., 1998), pigeon (Dickman, 1996), rabbit (Ezure and Graf, 1984; Mazza and Winterson, 1984), guinea pig (Curthoys et al., 1975), and chinchilla (Hullar and Williams, 2006), while in others such as rat (Blanks and Torigoe, 1989) and cat (Blanks et al., 1972) differences are small. Non-orthogonal ipsilateral semicircular canals may result in increased sensitivity to motion in particular directions (Mazza and Winterson, 1984; Brichta et al., 1988; Hullar and Williams, 2006); however, experimental support for this view is conflicting. For example, in *Chinchilla* the semicircular canals are non-orthogonal, yet this rodent seems equally sensitive to rotations in all directions (Hullar and Williams, 2006). Each pair of synergistically acting canals forms a functional unit, following the push/pull operational mode that occurs when one canal becomes excited, such that its coplanar counterpart becomes inhibited (Blanks et al., 1972, 1985; Graf, 1988). Theoretically, the synergistically acting pairs should be coplanar or parallel (Blanks et al., 1972, 1985; Graf, 1988). Although they typically do not diverge greatly from the ideal condition within vertebrates (Blanks et al., 1972, 1985; Graf, 1988), synergistically acting semicircular canals were reported to deviate significantly from parallel in some mammals such as chinchilla,

guinea pig, rabbit, and cat (Curthoys et al., 1975; Ezure and Graf, 1984; Hullar and Williams, 2006).

Only very limited data on these orientation angles are available for primates. Macaques have a large angular offset (98.7°) between the ipsilateral anterior and lateral semicircular canals, whereas in squirrel monkeys the canals are nearly orthogonal (90.4°, Blanks et al., 1985). The angles between the anterior and posterior, and posterior and lateral semicircular canals of these two anthropoids are very nearly orthogonal (Blanks et al., 1985). In both of those taxa, the synergistic vertical semicircular canal pairs all deviate from parallel by more than 10° (Blanks et al., 1985; Reisine et al., 1988). The two lateral canals in macaques are nearly parallel, whereas in squirrel monkeys the two canals form an angle of more than 15° (Blanks et al., 1985; Reisine et al., 1988). The orientation of the semicircular canals in *Chilecebus carrascoensis* closely mirrors that of these two extant anthropoid primates. As no functional interpretation has yet been linked to the differences in orientation angles between macaque and squirrel monkey, the resemblances and differences to *Chilecebus carrascoensis* cannot cast any light on functional predictions in this fossil taxon at this time.

When ASCm < PSCm is used to represent the planar angle of the ipsilateral VSC, and the sum of the angles of ASCm < SG and PSCm < SG represents the planar angle of the synergistically acting VSC pair, a wider comparison can be made among extant primates (Fig. 8). The two angles of *Chilecebus carrascoensis* are very close to those of *Mandrillus sphinx*. However, this similarity may not reflect similar locomotor patterns since similarity of these angles does not always correlate closely with similar locomotor patterns. For example, *Cebus paella*, *Hylobates pileatus*, and *Hylobates syndactylus* group closely in Figure 8 despite evident locomotor differences.

Principal component analysis, factor analysis, and similarity groups

Primates exhibit substantial variation in the dimensions, proportions, shapes, planarity, and orientations of the semicircular canals, and these features do not vary independently of one another. The PCA and FA in this study indicate that the orientations of the bony labyrinth, particularly the orientation of the lateral semicircular canal, contribute to the majority of the observed variance. As shown previously (Spoor and Zonneveld, 1998), the orientation of the lateral semicircular canal and some shape variables, such as the sagittal labyrinth index and the torsion of the posterior semicircular canals, covary closely with the bony labyrinth orientations and the cranial floor angle (Table 3).

The relative size of the semicircular canal accounts for little of the total variance. One reason could be that the dimensional variance in the bony labyrinth is less than the variance in its spatial orientation. Therefore, when the orientation and dimension variables are pooled into a single analysis, variation in orientation will overshadow the dimensional variance. Another possible explanation is the limited available taxonomic and locomotor mode sampling among taxa. Taxa with extreme locomotor patterns, such as the agile jumping tarsiers and the cautious slow climbing lorises, cannot be included due to inadequate published data. Therefore, the actual variances of some variables across primates, especially the relative size of the semicircular canals, may be inadequately reflected in our analysis.

Although taxa with distinctive locomotor patterns, such as *Alouatta seniculus* and *Lagothrix lagothricha*, *Indri indri* and *Propithecus diadema*, "great apes," gibbons, and humans could all be set apart from the others using rescaled Euclidean distance data (Fig. 9), the clustering does not precisely correlate with locomotor patterns, particularly for quadrupedal walking and climbing monkeys. It is conceivable, therefore, that the sizes, proportions, and orientations of the bony labyrinth do not correspond closely with locomotor patterns. Many morphological and physiological studies suggest that these variables are related to the afferent sensitivity (precisely how they are correlated causally is actually debatable); however, their relationship to locomotor pattern has yet to be fully/sufficiently evaluated. The limitations of taxon sampling also cloud current interpretations, with data from only 22 extant taxa available for this analysis.

Regarding the position of *Chilecebus carrascoensis* within the similarity matrix, Figure 9 underscores its general resemblance to quadrupedal monkeys, including *Cebus apella* and *Saimiri sciureus*. Nevertheless, because it is not positioned especially near any single living taxon, we must for the moment consider it to be unique in its combination of labyrinth characteristics (and inferred suite of locomotor correlations). Unless *Chilecebus carrascoensis* is extremely autapomorphic and specialized relative to all other anthropoids, its closest resemblance ultimately will lie either with: 1) early fossil anthropoids, if its morphology reflects retention of ancestral anthropoid (or deeper primate) conditions, 2) some other small-bodied living or fossil platyrrhine that remains to be evaluated or discovered, if phylogeny is the dominant influence on labyrinth morphology (augmented by at least some functional constraints, in that the Platyrrhini are entirely arboreal), or 3) some suite of primate taxa with common functional attributes that can be shown to covary closely with labyrinth morphology through increased taxon and locomotor style sampling.

Summary

The dimensions, proportions, shape ratios, orientations, and torsion angles of the bony labyrinth of *Chilecebus carrascoensis* fall within the range of variation observed in previously studied extant primates. Semicircular canal dimensions have long been suggested to correlate closely with equilibrial sensitivity and locomotor patterns. However, the precision of such correlations remains uncertain. A score of about 3–4 on the agility scale of Spoor et al. (2007) would be predicted for *Chilecebus carrascoensis*. However, when considering the ambiguity of agility cataloging and the broad overlap of agility scores among mammals with different semicircular canal sizes, such an estimator of agility cannot link semicircular canal size to any specific locomotor pattern. Variations in proportions, shape indices, and orientations of the semicircular canals of extant primates show some signals that might be correlated with phylogenetic or functional factors. The available data suggest that no single shape, proportion, or orientation variable plays a primary role in determining the locomotor patterns. Principle Component Analysis (PCA) and Factor Analysis (FA) reveal that many of these variables are highly correlated. Some variables, such as the orientation of the lateral semicircular canal, contribute more than relative semicircular canal size, although the latter has been widely proposed to be correlated with equilibrial sensitivity, agility, and locomotor patterns. A similarity matrix based on PCA scores shows that the primates in the analysis can be clustered, although not precisely, into several groups. *Chilecebus carrascoensis* shows relatively greater similarity to a diversity of taxa, including many generalized quadrupedal "monkeys." The same data indicate that *Chilecebus carrascoensis* was not a suspensory brachiating or slow climbing monkey and that its closest analog may lie with some other small-bodied living or fossil platyrrhine that remains to be evaluated or discovered.

Acknowledgements

This research was supported by our home institutions, The Field Museum (Chicago), research grants from the U.S. National Science Foundation (DEB-9317943, DEB-0317014 and DEB-0513476 to JJF;

DEB-9020213 and DEB-9318126 to ARW; DGE-0333415 to XN), a John S. Guggenheim Memorial Foundation Fellowship (to JJF), and the Chinese National Science Foundation (40672009 to XN). For the CT scanning of *Chilecebus carrascoensis*, we thank Drs. Timothy Ryan and Alan Walker of Penn State University and the PSU Center for Quantitative Imaging. We are grateful for the long term support of the Museo Nacional de Historia Natural (Santiago, Chile) and the Consejo Nacional de Monumentos Naturales de Chile. We appreciate the anonymous reviewers' thorough, extensive, and critical commentary, and the editor's advice for revisions.

References

Baxter, B.S., Sorenson, J.A., 1981. Factors affecting the measurement of size and CT number in computed tomography. Invest. Radiol. 16 (4), 337–341.

Blanks, R.H., Curthoys, I.S., Markham, C.H., 1972. Planar relationships of semicircular canals in the cat. Am. J. Physiol. 223 (1), 55–62.

Blanks, R.H., Curthoys, I.S., Markham, C.H., 1975a. Planar relationships of the semicircular canals in man. Acta Otolaryngol. 80 (3–4), 185–196.

Blanks, R.H., Estes, M.S., Markham, C.H., 1975b. Physiologic characteristics of vestibular first-order canal neurons in the cat. II. Response to constant angular acceleration. J. Neurophysiol. 38 (5), 1250–1268.

Blanks, R.H.I., Curthoys, I.S., Bennett, M.L., Markham, C.H., 1985. Planar relationships of the semicircular canals in rhesus and squirrel monkeys. Brain Res. 340 (2), 315–324.

Blanks, R.H.I., Torigoe, Y., 1989. Orientation of the semicircular canals in rat. Brain Res. 487 (2), 278–287.

Brichta, A.M., Acuña, D.L., Peterson, E.H., 1988. Planar relations of semicircular canals in awake, resting turtles, *Pseudemys scripta*. Brain Behav. Evol. 32 (4), 236–245.

de Burlet, H.M., 1934. Vergleichende Anatomie des stato-akustischen Organs. a) Die innere Ohrsphäre. Zweiter Band, 2. Hälfte. In: Bolk, L., Göppert, E., Kallius, E., Lubosch, W. (Eds.), Handbuch der vergleichenden Anatomie der Wirbeltiere. Urban and Schwarzenberg, Berlin, Wien, pp. 1293–1380.

Clarke, A.H., 2005. On the vestibular labyrinth of *Brachiosaurus brancai*. J. Vestib. Res. 15, 65–71.

Clauser, D.A., 1980. Functional and Comparative Anatomy of the Primate Spinal Column: Some Postural and Locomotor Adaptations. University of Wisconsin, Milwaukee.

Curthoys, I.S., Curthoys, E.J., Blanks, R.H., Markham, C.H., 1975. The orientation of the semicircular canals in the guinea pig. Acta Otolaryngol. 80 (3–4), 197–205.

Curthoys, I.S., Blanks, R.H.I., Markham, C.H., 1977. Semicircular canal radii of curvature (R) in cat, guinea pig, and man. J. Morphol. 151 (1), 1–15.

Dickman, J.D., 1996. Spatial orientation of semicircular canals and afferent sensitivity vectors in pigeons. Exp. Brain Res. 111 (1), 8–20.

Ezure, K., Graf, W., 1984. A quantitative analysis of the spatial organization of the vestibulo-ocular reflexes in lateral- and frontal-eyed animals—I. Orientation of semicircular canals and extraocular muscles. Neuroscience 12 (1), 85–93.

Flynn, J.J., Wyss, A.R., Charrier, R., Swisher, C.C., 1995. An Early Miocene anthropoid skull from the Chilean Andes. Nature 373 (6515), 603–607.

Ghanem, T.A., Rabbitt, R.D., Tresco, P.A., 1998. Three-dimensional reconstruction of the membranous vestibular labyrinth in the toadfish, *Opsanus tau*. Hear. Res. 124 (1–2), 27–43.

Graf, W., 1988. Motion detection in physical space and its peripheral and central representation. Ann. N.Y. Acad. Sci. 545, 154–169.

Graf, W., Vidal, P.-P., 1996. Semicircular canal size and upright stance are not interrelated. J. Hum. Evol. 30 (2), 175–181.

Gray, A.A., 1907. The Labyrinth of Animals, including Mammals, Birds, Reptiles and Amphibians, vol. 1. J. and A. Churchill, London.

Gray, A.A., 1908a. An investigation on the anatomical structure and relationships of the labyrinth in the reptile, the bird, and the mammal. Proc. R. Soc. Lond. B. Biol. Sci. 80 (543), 507–528.

Gray, A.A., 1908b. The Labyrinth of Animals, including Mammals, Birds, Reptiles and Amphibians, vol. 2. J. and A. Churchill, London.

Hadžiselimović, H., Savković, L.J., 1964. Appearance of semicircular canals in birds in relation to mode of life. Acta Anat. 57, 306–315.

Howland, H.C., Masci, J., 1973. The phylogenetic allometry of the semicircular canals of small fishes. Zoomorphology 75 (4), 283–296.

Hullar, T.E., 2006. Semicircular canal geometry, afferent sensitivity, and animal behavior. Anat. Rec. 288A (4), 466–472.

Hullar, T.E., Williams, C.D., 2006. Geometry of the semicircular canals of the chinchilla (*Chinchilla laniger*). Hear. Res. 213 (1–2), 17–24.

Jeffery, N., Ryan, T.M., Spoor, F., 2008. The primate subarcuate fossa and its relationship to the semicircular canals part II: adult interspecific variation. J. Hum. Evol. 55, 326–339.

Jones, G.M., Spells, K.E., 1963. A theoretical and comparative study of the functional dependence of the semicircular canal upon its physical dimensions. Proc. R. Soc. Lond. B. Biol. Sci. 157 (968), 403–419.

Lindenlaub, T., Burda, H., Nevo, E., 1995. Convergent evolution of the vestibular organ in the subterranean mole-rats, *Cryptomys* and *Spalax*, as compared with the aboveground rat, *Rattus*. J. Morphol. 224 (3), 303–311.

Manoussaki, D., Chadwick, R.S., Ketten, D.R., Arruda, J., Dimitriadis, E.K., 2008. The influence of cochlear shape on low-frequency hearing. Proc. Natl. Acad. Sci. U.S.A 105 (16), 6162–6166.

Matano, S., Kubo, T., Günther, M., 1985. Semicircular canal organ in three primate species and behavioural correlations. Fortschr. Zool. 30, 677–680.

Matano, S., Kubo, T., Matsunaga, T., Niemitz, C., Gunther, M., 1986. On size of the semicircular canals organ in the *Tarsius bancanus*. In: Taub, D.M., King, F.A. (Eds.), Current Perspectives in Primate Biology. Van Nostrand Reinhold Company, New York, pp. 122–129.

Mazza, D., Winterson, B.J., 1984. Semicircular canal orientation in the adult resting rabbit. Acta Otolaryngol. 98 (5–6), 472–480.

McVean, A., 1999. Are the semicircular canals of the European mole, *Talpa europaea*, adapted to a subterranean habitat? Comp. Biochem. Physiol., Part A Mol. Integr. Physiol. 123, 173–178.

Meng, J., Wyss, A.R., 1995. Monotreme affinities and low-frequency hearing suggested by multituberculate ear. Nature 377 (6545), 141–144.

Reisine, H., Simpson, J.I., Henn, V., 1988. A geometric analysis of semicircular canals and induced activity in their peripheral afferents in the rhesus monkey. Ann. N.Y. Acad. Sci. 545, 10–20.

Sears, K.E., Finarelli, J.A., Flynn, J.J., Wyss, A.R., 2008. Estimating body mass in new world "monkeys" (Platyrrhini, Primates), with a consideration of the Miocene platyrrhine, *Chilecebus carrascoensis*. Am. Mus. Novit. 3617, 1–29.

Silcox, M.T., Bloch, J.I., Boyer, D.M., Godinot, M., Ryan, T.M., Spoor, F., Walker, A., 2009. Semicircular canal system in early primates. J. Hum. Evol. 56 (3), 315–327.

Smith, R.J., Jungers, W.L., 1997. Body mass in comparative primatology. J. Hum. Evol. 32 (6), 523–559.

Spoor, C.F., Zonneveld, F.W., Macho, G.A., 1993. Linear measurements of cortical bone and dental enamel by computed tomography: applications and problems. Am. J. Phys. Anthropol. 91 (4), 469–484.

Spoor, F., Wood, B., Zonneveld, F., 1994. Implications of early hominid labyrinthine morphology for evolution of human bipedal locomotion. Nature 369 (6482), 645–648.

Spoor, F., Wood, B., Zonneveld, F., 1996. Evidence for a link between human-semicircular canal size and bipedal behaviour. J. Hum. Evol. 30 (2), 183–187.

Spoor, F., Bajpai, S., Hussain, S.T., Kumar, K., Thewissen, J.G.M., 2002. Vestibular evidence for the evolution of aquatic behaviour in early cetaceans. Nature 417 (6885), 163–166.

Spoor, F., Garland Jr., T., Krovitz, G., Ryan, T.M., Silcox, M.T., Walker, A., 2007. The primate semicircular canal system and locomotion. Proc. Natl. Acad. Sci. 104 (26), 10808–10812.

Spoor, F., Zonneveld, F., 1995. Morphometry of the primate bony labyrinth: a new method based on high-resolution computed tomography. J. Anat. 186, 271–286.

Spoor, F., Zonneveld, F., 1998. Comparative review of the human bony labyrinth. Yearb. Phys. Anthropol. 41, 211–251.

Stebbins, W.C., 1978. Hearing of the primates. In: Chivers, D.J., Herbert, J. (Eds.), Recent Advances in Primatology. Behaviour, vol. 1. Academic Press, London; New York, pp. 705–720.

Stebbins, W.C., 1980. The evolution of hearing in the mammals. In: Popper, A.N., Fay, R.R. (Eds.), Comparative Studies of Hearing in Vertebrates. Springer-Verlag, New York, pp. 421–436.

Steinhausen, W., 1933. Über die Beobachtung der Cupula in den Bogengangsampullen des Labyrinths des lebenden Hechts. Pflugers Arch. Gesamte Physiol. Menschen Tiere 232 (1), 500–512.

Takahashi, H., 1976. A comparative anatomical study of the bony labyrinth of the inner ear in primates. Acta Anatomica Nipponica 51 (5), 366–387.

Ten Kate, J.H., Van Barneveld, H.H., Kuiper, J.W., 1970. The dimensions and sensitivities of semicircular canals. J. Exp. Biol. 53 (2), 501–514.

Walker, A., Ryan, T.M., Silcox, M.T., Simons, E.L., Spoor, F., 2008. The semicircular canal system and locomotion: the case of extinct lemuroids and lorisoids. Evol. Anthropol. 17 (3), 135–145.

Watt, H.J., 1917. The typical form of the cochlea and its variations. Proc. R. Soc. Lond., B, Biol. Sci. 89 (618), 410–421.

Werner, C.F., 1960. Mittel- und Innenohr. In: Hofer, H., Schultz, A.H., Starck, D. (Eds.), Primatologia, Handbuch der Primatenkunde. Teil 1, Lieferung 5: Das Ohr, vol. 2. S. Karger, Basel, pp. 1–40.

West, C.D., 1985. The relationship of the spiral turns of the cochlea and the length of the basilar membrane to the range of audible frequencies in ground dwelling mammals. J. Acoust. Soc. Am. 77 (3), 1091–1101.

Wyss, A.R., Flynn, J.J., 1994. "Anthropoidea": a name, not an entity. Evol. Anthropol. 3 (6), 187–188.

Yang, A., Hullar, T.E., 2007. Relationship of semicircular canal size to vestibular-nerve afferent sensitivity in mammals. J. Neurophysiol. 98 (6), 3197–3205.

Zonneveld, F.W. (Ed.), 1987. Computed Tomography of the Temporal Bone and Orbit. Urban and Schwarzenberg, Baltimore.